Science and Technology Publishing (SCI & TECH)
ISSN: 2632-1017
Vol. 6 Issue 7, July - 2022

Design Of Computer Program For Assessment Of The Impact Of Satellite Antenna Pointing Error On The Effective Parabolic Antenna Gain And Aperture Diameter

Young, Emem Godwin[1]
Department of Computer Engineering
Akwa Ibom State Polytechnic , Ikot Osurua Ikot Ekpene

Uduak Etim Udoka[2]
Department of Computer Engineering
Akwa Ibom State Polytechnic , Ikot Osurua Ikot Ekpene

Usoh , Midighe Abraham[3]
Department of Computer Engineering
Akwa Ibom State Polytechnic , Ikot Osurua Ikot Ekpene

***Abstract*— The design of computer program for assessment of the impact of satellite antenna pointing error on the effective parabolic antenna gain and aperture diameter is presented. The program also implemented parametric analysis of the effect of signal frequency on the antenna gain, effective aperture diameter for different antenna pointing errors. The mathematical expressions for the computations were presented along with the design of the program algorithm. The program was implemented in Visual Basic for Application. Sample numerical examples were presented with antenna efficiency of 0.65, parabolic antenna diameter of 1.2 m, antenna pointing error range of 0 ° to 0.5° and frequency range of 100 MHz to 2100 MHz. The program results were presented in tables and graphs with trend line fitted on the graphs. In all, the program results provides comprehensive analysis of the impact of the antenna pointing error and frequency on the key parameters of the parabolic antenna.**

Keywords — Antenna Gain , Pointing Error , Aperture Diameter, Satellite Antenna, Parabolic Antenna

1. Introduction

Satellite communications operates mainly in the microwave frequency band which works best under line-of-sight conditions [1,2,3,4,5,6,7,8,9,10,11]. In this case, there should be clear line-of-sight between the transmitter antenna and the receiver antenna [12,13, 14,15, 16,17, 18, 19, 20]. When parabolic antenna is used, the parabolic antenna will focus and direct the transmitted signal along the line-of-sight to the receiving parabolic antenna [21,22,23,24,25,26,27,28]. Accurate alignment of the transmitting and receiving antennas is essential for maximum signal power reception at the receiver [29,30,31,32,33,34].

In some cases, there is antenna pointing error which cause some losses in the effective antenna gain [35,36,37,38,39,40,41,42,43,44,45]. Hence, the actual antenna gain obtained when there is no pointing error is different from the antenna gain when there is pointing error. The difference in antenna gain also means that the effective parabolic antenna diameter is also affected. Hence, this paper is mean to present the development and application of a computer program for assessing the impact of pointing error on the effective antenna gain of parabolic antenna in the presence of pointing error, the effective antenna diameter with pointing error and other relevant parameters associated with antenna pointing error. The detailed algorithm for the program is presented along with numerical examples showing the applicability of the program.

2. Methodology

2.1 The mathematical expressions parametric analysis of impact of satellite antenna pointing error

When a parabolic antenna is designed for a signal with λ wavelength in meters, if the parabolic antenna has d_{mx} diameter in meters and efficiency of η, then, the antenna gain, $G_{mx(dB)}$ in dB is given by;

$$G_{mx(dB)} = 10Log\left((\pi^2)\eta\left(\frac{d_{mx}}{\lambda}\right)^2\right) \quad (1)$$

$$G_{mx(dB)} = 9.942997 + 10Log(\eta) + 20Log\left(\frac{d_{mx}}{\lambda}\right) \quad (2)$$

The θ_{3dB} antenna beam width is expressed as;

$$\theta_{3dB} = 70\left(\frac{\lambda}{d_{mx}}\right) = 70\left(\frac{3x10^8}{(f)d_{mx}}\right) \quad (3)$$

Where the f is given in Hz. If there is antenna pointing error of θ, then , the pointing loss, L_θ of the antenna is expressed as;

$$L_\theta = 12\left(\frac{\theta}{\theta_{3dB}}\right)^2 = 12\left(\frac{\theta}{70}\left(\frac{\lambda}{d_{mx}}\right)\right)^2 \quad (4)$$

The effective antenna gain, $G_{e(dB)}$ is computed as;

$$G_{e(dB)} = G_{mx(dB)} - L_\theta \quad (5)$$

$$G_{e(dB)} = 10\,Log\left((\pi^2)\eta\left(\frac{\lambda}{d_{mx}}\right)^2\right) - 12\left(\frac{\theta}{70}\left(\frac{\lambda}{d_{mx}}\right)\right)^2 \quad (6)$$

The diameter, D_e for the effective antenna gain, $G_{e(dB)}$ is computed as;

$$D_e = \lambda\sqrt{\frac{10^{\left(\frac{G_{e(dB)}}{10}\right)}}{(\pi^2)\eta}} \quad (7)$$

Change in antenna diameter, Δd is given as;

$$\Delta d = d_{mx} - d_e \quad (8)$$

Algorithm 1 The procedure for the Module Main ()

Algorithm 1 The procedure for the Module Main ()

```
Module Main ()
  1:Input SelectParam /* Select the parametric to be used for the analysis ; Integer 1 to 5
                      '1' for parametric analysis using (λ)
                      '2' for parametric analysis using (f)
                      '3' for parametric analysis using (η)
                      '4' for parametric analysis using (d_mx)
                      '5' for parametric analysis using (θ)
                      */
  2:If SelectParam = 1 Then
  3:   Module 1 ParAnal_using_λ
  4: ElseIf SelectParam = 2 Then
  5:   Module 2 ParAnal_using_f
  6:ElseIf SelectParam = 3 Then
  7:   Module 3 ParAnal_using_η
  8: ElseIf SelectParam = 4 Then
  9: Module 4 ParAnal_using_d_mx
  10:Else
  11: Module 5 ParAnal_using_θ
  12:EndIf
  13: End Module main
```

Algorithm 2 The procedure for the Module 1 ParAnal_using_λ ()

Algorithm 2 The procedure for the Module 1 ParAnal_using_λ ()

```
Module 1 ParAnal_using_λ ()
1: Input λ_L // lower value of wavelength
2: Input λ_H // higher value of wavelength
3: Input n_x // number of steps to cover the range λ_L to λ_H
4: Declare the following arrays λ[n_x], G_mx(dB)[n_x], θ_3dB[n_x], L_θ [X], G_e(dB)[n_x], d_e[n_x],
                                Δd[n_x]
5: Input η
6: Input d_mx
7: Input θ
8: Declare the following arrays η[n_x], d_mx[n_x], θ[n_x]
9: For X = 1 , X ( n_x, X = X + 1
10: λ[X] = X((λ_H − λ_L)/n_x)
11: η[X] = η
12: d_mx[X] = d_mx
```

2.2 The program procedures for the parametric analysis of impact of satellite antenna pointing error

The general procedure for computing the parameters of the parabolic antenna with a pointing error can be designed to comprise of a main module and other several other submodules based on the specific input parameter upon which the parametric analysis is being conducted.

13: $\theta[\mathrm{X}] = \theta$

14: Compute $G_{\mathrm{mx}(dB)}[\mathrm{X}] = 10Log\left((\pi^2)\eta[\mathrm{X}]\left(\frac{\mathrm{d}_{mx}[\mathrm{X}]}{\lambda}\right)^2\right)$ using equation (1)

15: Compute $\theta_{3dB}[\mathrm{X}] = 70\left(\frac{\lambda[\mathrm{X}]}{\mathrm{d}_{mx}[\mathrm{X}]}\right)$ using equation (3)

16: Compute $L_\theta[\mathrm{X}] = 12\left(\frac{\theta[\mathrm{X}]}{70}\left(\frac{\lambda[\mathrm{X}]}{\mathrm{d}_{mx}[\mathrm{X}]}\right)\right)^2$ using equation (4)

17: Compute $G_{e(dB)}[\mathrm{X}] = G_{mx(dB)}[\mathrm{X}] - L_\theta[\mathrm{X}]$ using equation (5)

18: Compute $d_e[\mathrm{X}] = \lambda[\mathrm{X}]\sqrt{\frac{10^{\left(\frac{G_{e(dB)}[\mathrm{X}]}{10}\right)}}{(\pi^2)\eta[\mathrm{X}]}}$ using equation (7)

19: Compute $\Delta\mathrm{d}[\mathrm{X}] = \mathrm{d}_{mx}[\mathrm{X}] - d_e[\mathrm{X}]$ using equation (8)

20: Output $\lambda[n_x]$, $\eta[\mathrm{X}]$, $\mathrm{d}_{mx}[\mathrm{X}]$, $\theta[\mathrm{X}]$, $G_{\mathrm{mx}(dB)}[n_x]$, $\theta_{3dB}[n_x]$, $L_\theta[\mathrm{X}]$, $G_{e(dB)}[n_x]$, $d_e[n_x]$, $\Delta\mathrm{d}[n_x]$

21: Next For Loop

22: End For Loop

23: End Module 1 ParAnal_using_λ ()

Algorithm 3 The procedure for the Module 2 ParAnal_using_f()

Algorithm 3 The procedure for the Module 2 ParAnal_using_f()

Module 2 ParAnal_using_f()

1: Input f_L // lower value of frequency in Hz

2: Input f_H // higher value of frequency in Hz

3: Input n_x // number of steps to cover the range f_L to f_H

4: Declare the following arrays $\lambda[n_x]$, $G_{\mathrm{mx}(dB)}[n_x]$, $\theta_{3dB}[n_x]$, $L_\theta[\mathrm{X}]$, $G_{e(dB)}[n_x]$, $d_e[n_x]$, $\Delta\mathrm{d}[n_x]$

5: Input η

6: Input d_{mx}

7: Input θ

8: Declare the following arrays $\eta[n_x]$, $\mathrm{d}_{mx}[n_x]$, $\theta[n_x]$

9: For X = 1 , X (n_x, $X = \mathrm{X} + 1$

10: $f[\mathrm{X}] = X\left(\frac{f_H - f_L}{n_x}\right)$

11: $\lambda[\mathrm{X}] = \left(\frac{3x10^8}{f[\mathrm{X}]}\right)$

12: $\eta[\mathrm{X}] = \eta$

13: $\mathrm{d}_{mx}[\mathrm{X}] = \mathrm{d}_{mx}$

14: $\theta[\mathrm{X}] = \theta$

15: Compute $G_{\mathrm{mx}(dB)}[\mathrm{X}] = 10Log\left((\pi^2)\eta[\mathrm{X}]\left(\frac{\mathrm{d}_{mx}[\mathrm{X}]}{\lambda}\right)^2\right)$ using equation (1)

16: Compute $\theta_{3dB}[\mathrm{X}] = 70\left(\frac{\lambda[\mathrm{X}]}{\mathrm{d}_{mx}[\mathrm{X}]}\right)$ using equation (3)

17: Compute $L_\theta[\mathrm{X}] = 12\left(\frac{\theta[\mathrm{X}]}{70}\left(\frac{\lambda[\mathrm{X}]}{\mathrm{d}_{mx}[\mathrm{X}]}\right)\right)^2$ using equation (4)

18: Compute $G_{e(dB)}[\mathrm{X}] = G_{mx(dB)}[\mathrm{X}] - L_\theta[\mathrm{X}]$ using equation (5)

19: Compute $d_e[\mathrm{X}] = \lambda[\mathrm{X}]\sqrt{\frac{10^{\left(\frac{G_{e(dB)}[\mathrm{X}]}{10}\right)}}{(\pi^2)\eta[\mathrm{X}]}}$ using equation (7)

20: Compute $\Delta\mathrm{d}[\mathrm{X}] = \mathrm{d}_{mx}[\mathrm{X}] - d_e[\mathrm{X}]$ using equation (8)

21: Output $f[\mathrm{X}]$, $\lambda[n_x]$, $\eta[\mathrm{X}]$, $\mathrm{d}_{mx}[\mathrm{X}]$, $\theta[\mathrm{X}]$, $G_{\mathrm{mx}(dB)}[n_x]$, $\theta_{3dB}[n_x]$, $L_\theta[\mathrm{X}]$, $G_{e(dB)}[n_x]$, $d_e[n_x]$, $\Delta\mathrm{d}[n_x]$

22: Next For Loop

23: End For Loop

24: End Module 2 ParAnal_using_f()

Algorithm 4 The procedure for the Module 3 ParAnal_using_η ( )

Algorithm 4 The procedure for the Module 3 ParAnal_using_η ( )

Module 3 ParAnal_using_η ( )
1: Input η_L // lower value of efficiency
2: Input η_H // higher value of efficiency
3: Input n_x // number of steps to cover the range η_L to η_H
4: Declare the following arrays $\Lambda[n_x]$, $G_{\mathrm{mx}(dB)}[n_x]$, $\theta_{3dB}[n_x]$, L_θ [X], $G_{e(dB)}[n_x]$, $d_e[n_x]$, $\Delta\mathrm{d}[n_x]$
5: Input Λ
6: Input d_{mx}
7: Input θ
8: Declare the following arrays $\eta[n_x]$, $\mathrm{d}_{mx}[n_x]$, $\theta[n_x]$
9: For X = 1 , X (n_x, $X = \mathrm{X} + 1$
10: $\eta[\mathrm{X}] = X\left(\frac{\eta_H - \eta_L}{n_x}\right)$
11: $\Lambda[\mathrm{X}] = \Lambda$
12: $\mathrm{d}_{mx}[\mathrm{X}] = \mathrm{d}_{mx}$
13: $\theta[\mathrm{X}] = \theta$
14: Compute $G_{\mathrm{mx}(dB)}[\mathrm{X}] = 10Log\left((\pi^2)\eta[\mathrm{X}]\left(\frac{\mathrm{d}_{mx}[\mathrm{X}]}{\Lambda}\right)^2\right)$ using equation (1)
15: Compute $\theta_{3dB}[\mathrm{X}] = 70\left(\frac{\Lambda[\mathrm{X}]}{\mathrm{d}_{mx}[\mathrm{X}]}\right)$ using equation (3)
16: Compute $L_\theta[\mathrm{X}] = 12\left(\frac{\theta[\mathrm{X}]}{70}\left(\frac{\Lambda[\mathrm{X}]}{\mathrm{d}_{mx}[\mathrm{X}]}\right)\right)^2$ using equation (4)
17: Compute $G_{e(dB)}[\mathrm{X}] = G_{mx(dB)}[\mathrm{X}] - L_\theta[\mathrm{X}]$ using equation (5)
18: Compute $d_e[\mathrm{X}] = \Lambda[\mathrm{X}]\sqrt{\frac{10^{\left(\frac{G_{e(dB)}[\mathrm{X}]}{10}\right)}}{(\pi^2)\eta[\mathrm{X}]}}$ using equation (7)
19: Compute $\Delta\mathrm{d}[\mathrm{X}] = \mathrm{d}_{mx}[\mathrm{X}] - d_e[\mathrm{X}]$ using equation (8)
20: Output $\Lambda[n_x]$, $\eta[\mathrm{X}]$, $\mathrm{d}_{mx}[\mathrm{X}]$, $\theta[\mathrm{X}]$, $G_{\mathrm{mx}(dB)}[n_x]$, $\theta_{3dB}[n_x]$, L_θ [X], $G_{e(dB)}[n_x]$, $d_e[n_x]$, $\Delta\mathrm{d}[n_x]$
21: Next For Loop
22: End For Loop
23: End Module 3 ParAnal_using_η ( )

Algorithm 5 The procedure for the Module 4 ParAnal_using_d_{mx} ( )

Algorithm 5 The procedure for the Module 4 ParAnal_using_d_{mx} ( )

Module 4 ParAnal_using_d_{mx} ( )
1: Input d_{mx_L} // lower value of antenna aperture diameter
2: Input d_{mx_H} // higher value of antenna aperture diameter
3: Input n_x // number of steps to cover the range d_{mx_L} to d_{mx_H}
4: Declare the following arrays $\Lambda[n_x]$, $G_{\mathrm{mx}(dB)}[n_x]$, $\theta_{3dB}[n_x]$, L_θ [X], $G_{e(dB)}[n_x]$, $d_e[n_x]$, $\Delta\mathrm{d}[n_x]$
5: Input Λ
6: Input η
7: Input θ
8: Declare the following arrays $\eta[n_x]$, $\mathrm{d}_{mx}[n_x]$, $\theta[n_x]$
9: For X = 1 , X (n_x, $X = \mathrm{X} + 1$

10: $\mathrm{d}_{mx}[\mathrm{X}] = X\left(\frac{\mathrm{d}_{mx_H} - \mathrm{d}_{mx_L}}{n_x}\right)$
11: $\lambda[\mathrm{X}] = \lambda$
12: $\eta[\mathrm{X}] = \eta$
13: $\theta[\mathrm{X}] = \theta$
14: Compute $G_{\mathrm{mx}(dB)}[\mathrm{X}] = 10Log\left((\pi^2)\eta[\mathrm{X}]\left(\frac{\mathrm{d}_{mx}[\mathrm{X}]}{\lambda}\right)^2\right)$ using equation (1)
15: Compute $\theta_{3dB}[\mathrm{X}] = 70\left(\frac{\lambda[\mathrm{X}]}{\mathrm{d}_{mx}[\mathrm{X}]}\right)$ using equation (3)
16: Compute $L_\theta[\mathrm{X}] = 12\left(\frac{\theta[\mathrm{X}]}{70}\left(\frac{\lambda[\mathrm{X}]}{\mathrm{d}_{mx}[\mathrm{X}]}\right)\right)^2$ using equation (4)
17: Compute $G_{e(dB)}[\mathrm{X}] = G_{mx(dB)}[\mathrm{X}] - L_\theta[\mathrm{X}]$ using equation (5)
18: Compute $d_e[\mathrm{X}] = \lambda[\mathrm{X}]\sqrt{\frac{10^{\left(\frac{G_{e(dB)}[\mathrm{X}]}{10}\right)}}{(\pi^2)\eta[\mathrm{X}]}}$ using equation (7)
19: Compute $\Delta\mathrm{d}[\mathrm{X}] = \mathrm{d}_{mx}[\mathrm{X}] - d_e[\mathrm{X}]$ using equation (8)
20: Output $\lambda[n_x]$, $\eta[\mathrm{X}]$, $\mathrm{d}_{mx}[\mathrm{X}]$, $\theta[\mathrm{X}]$, $G_{\mathrm{mx}(dB)}[n_x]$, $\theta_{3dB}[n_x]$, $L_\theta[\mathrm{X}]$, $G_{e(dB)}[n_x]$, $d_e[n_x]$, $\Delta\mathrm{d}[n_x]$
21: Next For Loop
22: End For Loop
23: End Module 4 ParAnal_using_d_{mx} ( )

Algorithm 6 The procedure for the Module 5 ParAnal_using_θ( )

Algorithm 6 The procedure for the Module 5 ParAnal_using_θ( )

Module 5 ParAnal_using_θ( )
1: Input θ_L // lower value of antenna pointing error
2: Input θ_H // higher value of antenna pointing error
3: Input n_x // number of steps to cover the range θ_L to θ_H
4: Declare the following arrays $\lambda[n_x]$, $G_{\mathrm{mx}(dB)}[n_x]$, $\theta_{3dB}[n_x]$, $L_\theta[\mathrm{X}]$, $G_{e(dB)}[n_x]$, $d_e[n_x]$, $\Delta\mathrm{d}[n_x]$
5: Input λ
6: Input η
7: Input d_{mx}
8: Declare the following arrays $\eta[n_x]$, $\mathrm{d}_{mx}[n_x]$, $\theta[n_x]$
9: For X = 1 , X (n_x, $X = \mathrm{X} + 1$
10: $\theta[\mathrm{X}] = X\left(\frac{\theta_H - \theta_L}{n_x}\right)$
11: $\lambda[\mathrm{X}] = \lambda$
12: $\eta[\mathrm{X}] = \eta$
13: $\mathrm{d}_{mx}[\mathrm{X}] = \mathrm{d}_{mx}$
14: Compute $G_{\mathrm{mx}(dB)}[\mathrm{X}] = 10Log\left((\pi^2)\eta[\mathrm{X}]\left(\frac{\mathrm{d}_{mx}[\mathrm{X}]}{\lambda}\right)^2\right)$ using equation (1)
15: Compute $\theta_{3dB}[\mathrm{X}] = 70\left(\frac{\lambda[\mathrm{X}]}{\mathrm{d}_{mx}[\mathrm{X}]}\right)$ using equation (3)
16: Compute $L_\theta[\mathrm{X}] = 12\left(\frac{\theta[\mathrm{X}]}{70}\left(\frac{\lambda[\mathrm{X}]}{\mathrm{d}_{mx}[\mathrm{X}]}\right)\right)^2$ using equation (4)
17: Compute $G_{e(dB)}[\mathrm{X}] = G_{mx(dB)}[\mathrm{X}] - L_\theta[\mathrm{X}]$ using equation (5)
18: Compute $d_e[\mathrm{X}] = \lambda[\mathrm{X}]\sqrt{\frac{10^{\left(\frac{G_{e(dB)}[\mathrm{X}]}{10}\right)}}{(\pi^2)\eta[\mathrm{X}]}}$ using equation (7)
19: Compute $\Delta\mathrm{d}[\mathrm{X}] = \mathrm{d}_{mx}[\mathrm{X}] - d_e[\mathrm{X}]$ using equation (8)
20: Output $\lambda[n_x]$, $\eta[\mathrm{X}]$, $\mathrm{d}_{mx}[\mathrm{X}]$, $\theta[\mathrm{X}]$, $G_{\mathrm{mx}(dB)}[n_x]$, $\theta_{3dB}[n_x]$, $L_\theta[\mathrm{X}]$, $G_{e(dB)}[n_x]$, $d_e[n_x]$, $\Delta\mathrm{d}[n_x]$
21: Next For Loop

```
22: End For Loop
23: End Module 5 ParAnal_using_θ( )
```

3. Results and discussion

The program was developed using Visual Basic for Applications that runs under Microsoft Excel platform. The program was used to conduct analysis on the impact of variations in one parameter of the antenna on anther. The results of the parametric analysis of the antenna loss versus antenna pointing error are shown in Table 1 and Figure 1, where Ƞ =0.65, dmx = 1.2 m and θ (deg) = 0.5º. The results show that the antenna loss increases with frequency and the increases is quadratic in respect of the frequency in MHz, as shown in Figure 1.

The results of the parametric analysis of the antenna gain with and without pointing loss versus frequency are shown in Table 2 and Figure 2, where Ƞ =0.65, dmx = 1.2 m and θ (deg) = 0.5º. The results show that the antenna gain without pointing loss, Gmx (dB) and effective antenna gain with pointing loss, Ge(dB) increase logarithmically with frequency but the of increase in Gmx (dB) is higher than that of Ge(dB). As such, as frequency increases, the difference between Gmx (dB) and Ge (dB) increases.

The results of the parametric analysis of the effective antenna diameter with pointing loss, de (m) versus frequency are shown in Table 3 and Figure 3, where Ƞ =0.65, dmx = 1.2 m and θ (deg) = 0.5º. The results show that de(m) decreases quadratically with frequency. As such, as frequency increases, the difference between dmx (m) and de (dB) increases.

The results of the parametric analysis of the antenna beam width, θ3dB versus frequency are shown in Table 4 and Figure 4, where Ƞ =0.65, dmx = 1.2 m and θ (deg) = 0.5º. The results show that θ3dB decreases inversely with frequency. As such, as frequency increases, the θ3dB increases

Table 1 The results of parametric analysis of the antenna loss versus antenna pointing error, where Ƞ =0.65, dmx = 1.2 m and θ (deg) = 0.5º

S/N	f (MHz)	Antenna Pointing Loss, Lθ (dB)	S/N	f (MHz)	Antenna Pointing Loss, Lθ (dB)
1	1000	0.010	11	11000	1.185
2	2000	0.039	12	12000	1.411
3	3000	0.088	13	13000	1.656
4	4000	0.157	14	14000	1.920
5	5000	0.245	15	15000	2.204
6	6000	0.353	16	16000	2.508
7	7000	0.480	17	17000	2.831
8	8000	0.627	18	18000	3.174
9	9000	0.793	19	19000	3.536
10	10000	0.980	20	20000	3.918
11	11000	1.185	21	21000	4.320

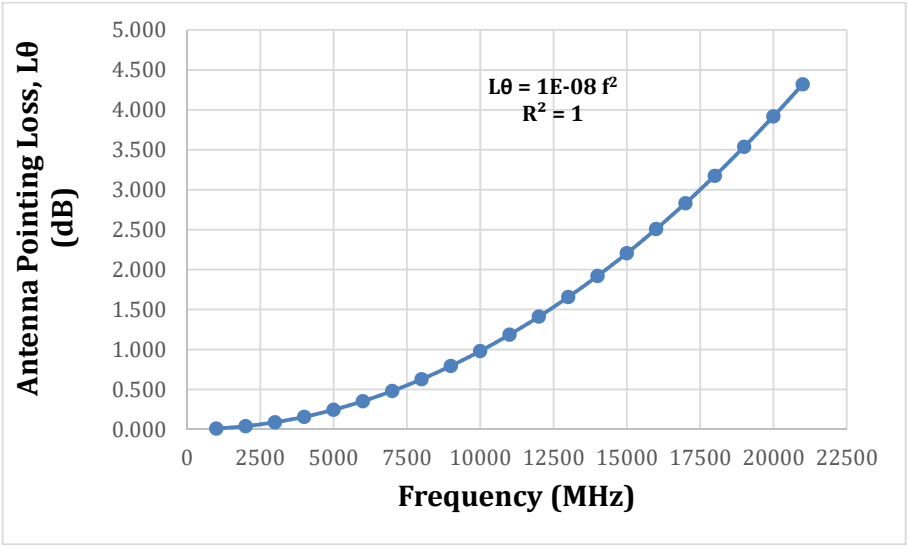

Figure 1 The graph of parametric analysis of the antenna loss versus antenna pointing error, where Ŋ =0.65, dmx = 1.2 m and θ (deg) = 0.5º

Table 2 The results of parametric analysis of the antenna gain with and without pointing loss versus frequency, where Ŋ =0.65, dmx = 1.2 m and θ (deg) = 0.5º

S/N	f (MHz)	Maximum Antenna Gain Without Pointing Loss, Gmx (dB)	Effective antenna gain with pointing loss, Ge(dB)	S/N	f (MHz)	Maximum Antenna Gain Without Pointing Loss, Gmx (dB)	Effective antenna gain with pointing loss, Ge(dB)
1	1000	20.113	20.104	11	11000	40.941	39.756
2	2000	26.134	26.095	12	12000	41.697	40.286
3	3000	29.656	29.568	13	13000	42.392	40.737
4	4000	32.155	31.998	14	14000	43.036	41.116
5	5000	34.093	33.848	15	15000	43.635	41.431
6	6000	35.676	35.324	16	16000	44.196	41.688
7	7000	37.015	36.535	17	17000	44.722	41.891
8	8000	38.175	37.548	18	18000	45.219	42.045
9	9000	39.198	38.405	19	19000	45.688	42.152
10	10000	40.113	39.134	20	20000	46.134	42.216
11	11000	40.941	39.756	21	21000	46.558	42.238

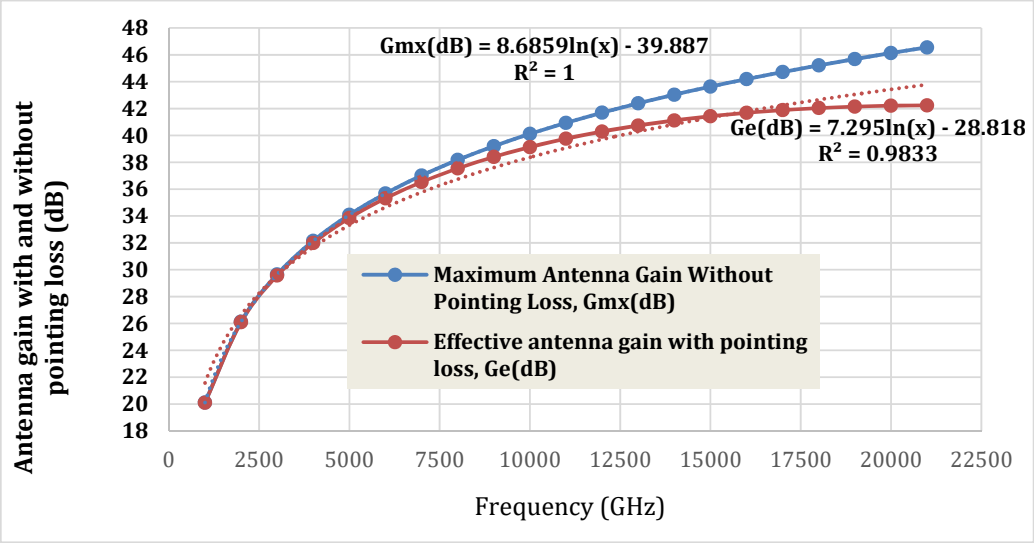

Figure 2 The graph of parametric analysis of the antenna gain with and without pointing loss versus frequency, where Ƞ =0.65, dmx = 1.2 m and θ (deg) = 0.5º

Table 3 The results of parametric analysis of the effective antenna diameter with pointing loss versus frequency, where Ƞ =0.65, dmx = 1.2 m and θ (deg) = 0.5º

S/N	f (MHz)	Actual antenna diameter without pointing loss, dmx (m)	Effective antenna diameter with pointing loss, de (m)	S/N	f (MHz)	Actual antenna diameter without pointing loss, dmx (m)	Effective antenna diameter with pointing loss, de (m)
1	1000	1.2	1.199	11	11000	1.2	1.047
2	2000	1.2	1.195	12	12000	1.2	1.02
3	3000	1.2	1.188	13	13000	1.2	0.992
4	4000	1.2	1.179	14	14000	1.2	0.962
5	5000	1.2	1.167	15	15000	1.2	0.931
6	6000	1.2	1.152	16	16000	1.2	0.899
7	7000	1.2	1.135	17	17000	1.2	0.866
8	8000	1.2	1.116	18	18000	1.2	0.833
9	9000	1.2	1.095	19	19000	1.2	0.799
10	10000	1.2	1.072	20	20000	1.2	0.764
11	11000	1.2	1.047	21	21000	1.2	0.73

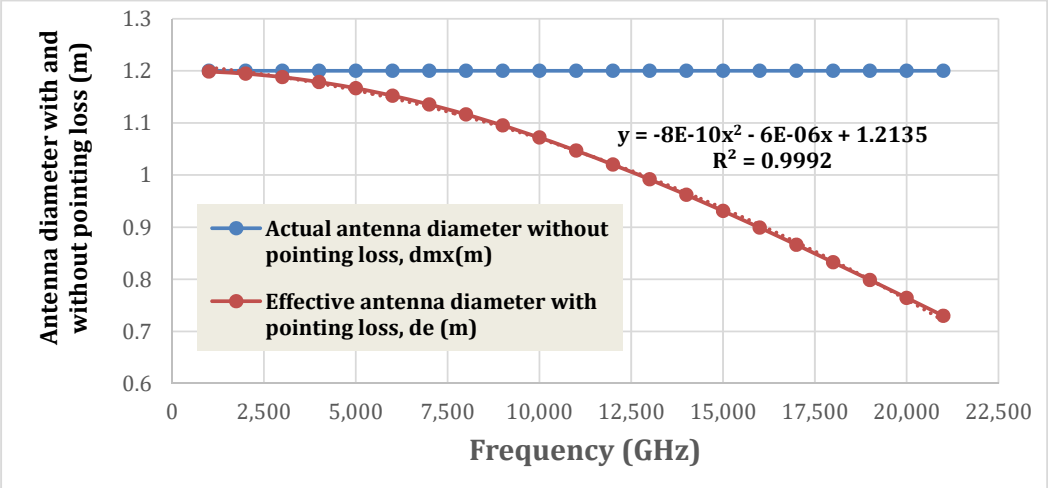

Figure 3 The graph of parametric analysis of the effective antenna diameter with pointing loss versus frequency, where Ƞ =0.65

Table 4 The results of parametric analysis of the antenna beam width, θ3dB versus frequency, where Ƞ =0.65, dmx = 1.2 m and θ (deg) = 0.5º

S/N	f (MHz)	Antenna beam width, θ3dB	S/N	f (MHz)	Antenna beam width, θ3dB
1	1000	17.500	11	11000	1.591
2	2000	8.750	12	12000	1.458
3	3000	5.833	13	13000	1.346
4	4000	4.375	14	14000	1.250
5	5000	3.500	15	15000	1.167
6	6000	2.917	16	16000	1.094
7	7000	2.500	17	17000	1.029
8	8000	2.188	18	18000	0.972
9	9000	1.944	19	19000	0.921
10	10000	1.750	20	20000	0.875
11	11000	1.591	21	21000	0.833

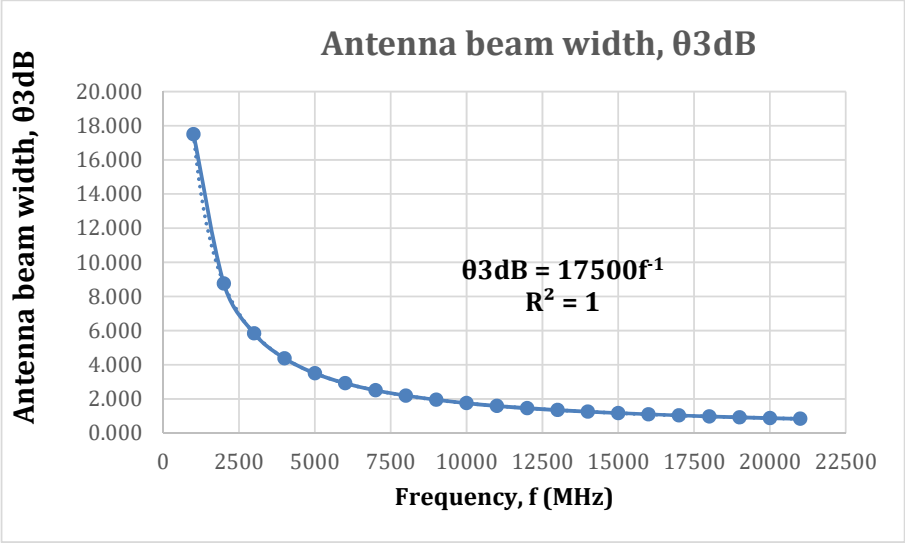

Figure 4 The graph of parametric analysis of the the antenna beam width, θ3dB versus frequency, where Ƞ =0.65, dmx = 1.2 m and θ (deg) = 0.5º

The results of the parametric analysis of the antenna pointing loss, Lθ versus antenna pointing error shown in Table 5 and Figure 5, where Ƞ =0.65, dmx = 1.2 m and f = 2000 MHz. The results show that the antenna pointing loss, Lθ increases quadratically with antenna pointing error, θ. As such, as θ increases, the antenna pointing loss, Lθ increases quadratically with θ in degrees.

The results of the parametric analysis of the effective antenna gain, Ge(dB) versus antenna pointing error are shown in Table 6 and Figure 6, where Ƞ =0.65, dmx = 1.2 m and f = 2000 MHz.. The results show that Ge(dB) decreases quadratically with frequency. As such, as θ increases, the effective antenna gain, Ge(dB) decreases quadratically with θ in degrees.

The results of the parametric analysis of the effective antenna diameter, de(m) versus antenna pointing error shown in Table 7 and Figure 7, where Ƞ =0.65, dmx = 1.2 m and f = 2000 MHz. The results show that the effective antenna diameter, de(m) decreases with third power of antenna pointing error, θ. As such, as θ increases, the effective antenna diameter, de(m) decreases with θ raised to power of 3.

Table 5 The parametric analysis of the antenna pointing loss versus antenna pointing error where Ƞ =0.65, dmx = 1.2 m and f = 2000 MHz

S/N	Antenna pointing error, θ (deg)	Antenna loss, Lθ (dB)	S/N	Antenna pointing error, θ (deg)	Antenna loss, Lθ (dB)
1	0	0	11	0.5	3.918
2	0.05	0.039	12	0.55	4.741
3	0.1	0.157	13	0.6	5.642
4	0.15	0.353	14	0.65	6.622
5	0.2	0.627	15	0.7	7.68
6	0.25	0.98	16	0.75	8.816
7	0.3	1.411	17	0.8	10.031
8	0.35	1.92	18	0.85	11.324
9	0.4	2.508	19	0.9	12.696
10	0.45	3.174	20	0.95	14.145
11	0.5	3.918	21	1	15.673

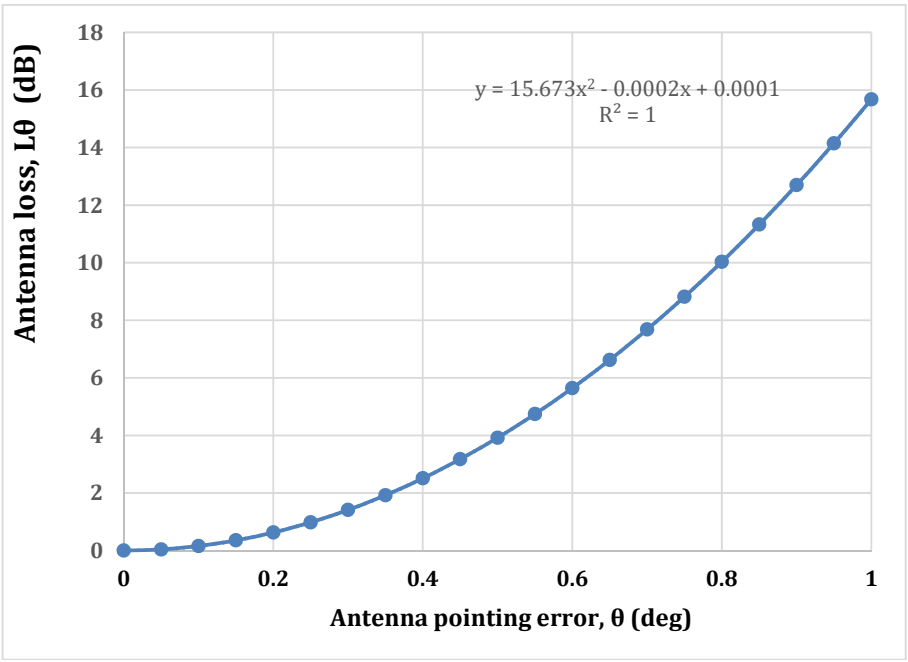

Figure 5 The graph of parametric analysis of the antenna pointing loss versus antenna pointing error where Ƞ =0.65, dmx = 1.2 m and f = 2000 MHz

Table 6 The parametric analysis of the effective antenna gain, Ge(dB) versus antenna pointing error where Ƞ =0.65, dmx = 1.2 m and f = 2000 MHz

S/N	Antenna pointing error, θ (deg)	Effective antenna gain with pointing loss, Ge(dB)	S/N	Antenna pointing error, θ (deg)	Effective antenna gain with pointing loss, Ge(dB)
1	0	46.134	11	0.5	42.216
2	0.05	46.095	12	0.55	41.393
3	0.1	45.977	13	0.6	40.491
4	0.15	45.781	14	0.65	39.512
5	0.2	45.507	15	0.7	38.454
6	0.25	45.154	16	0.75	37.318
7	0.3	44.723	17	0.8	36.103
8	0.35	44.214	18	0.85	34.81
9	0.4	43.626	19	0.9	33.438
10	0.45	42.96	20	0.95	31.989
11	0.5	42.216	21	1	30.46

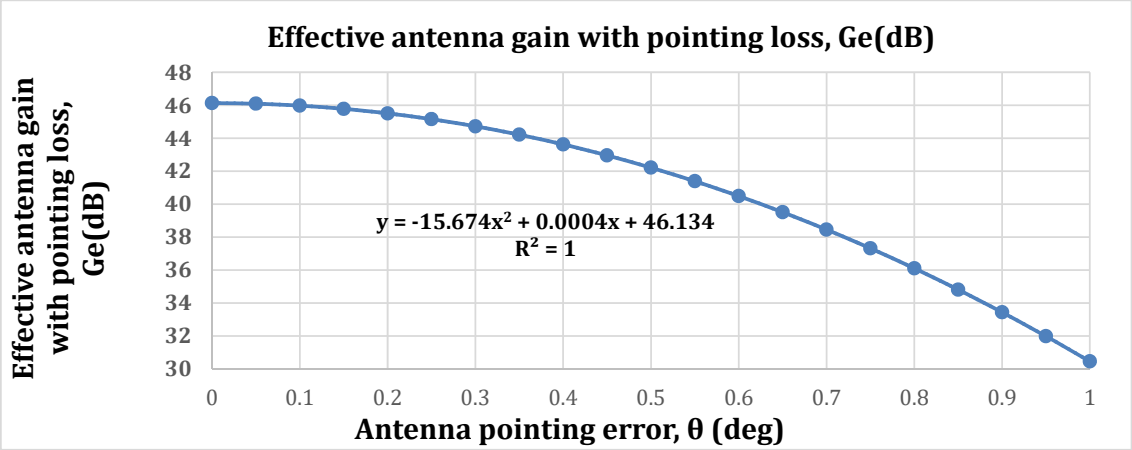

Figure 6 The graph of parametric analysis of the effective antenna gain, Ge(dB) versus antenna pointing error where Ƞ =0.65, dmx = 1.2 m and f = 2000 MHz

Table 7 The parametric analysis of the effective antenna diameter, de(m) versus antenna pointing error where Ƞ =0.65, dmx = 1.2 m and f = 2000 MHz

S/N	Antenna pointing error, θ (deg)	Effective antenna diameter with pointing loss, de (m)	S/N	Antenna pointing error, θ (deg)	Effective antenna diameter with pointing loss, de (m)
1	0	1.2	11	0.5	1.2
2	0.05	1.195	12	0.55	1.195
3	0.1	1.179	13	0.6	1.179
4	0.15	1.152	14	0.65	1.152
5	0.2	1.116	15	0.7	1.116
6	0.25	1.072	16	0.75	1.072
7	0.3	1.02	17	0.8	1.02
8	0.35	0.962	18	0.85	0.962
9	0.4	0.899	19	0.9	0.899
10	0.45	0.833	20	0.95	0.833
11	0.5	0.764	21	1	0.764

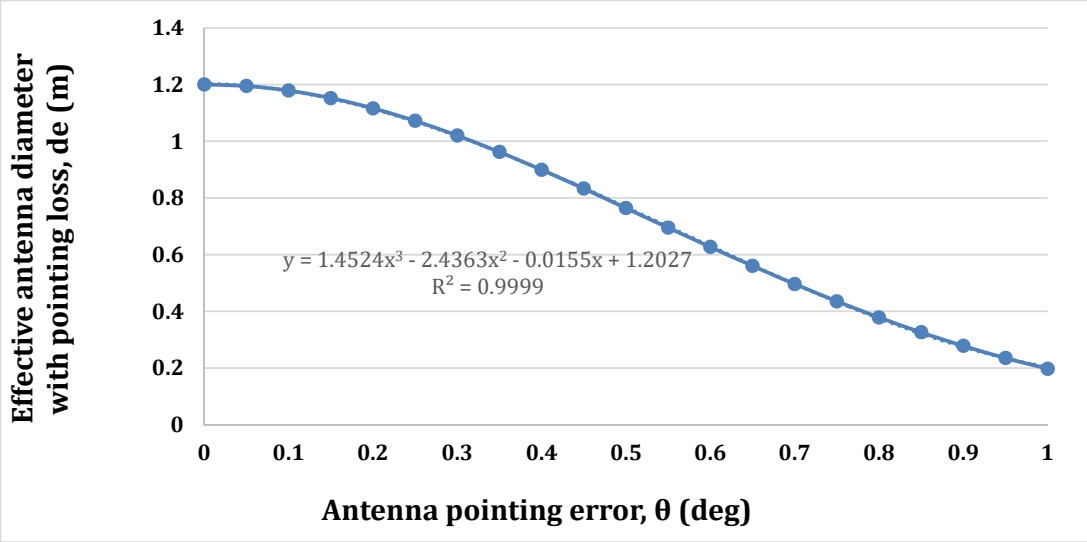

Figure 7 The graph of parametric analysis of the effective antenna diameter, de(m) versus antenna pointing error where Ƞ =0.65, dmx = 1.2 m and f = 2000 MHz

4. Conclusion

The program for parametric analysis of antenna pointing error impact on parabolic antenna gain, effective antenna diameter, and antenna pointing and beam width is presented. The program also captures the effect of frequency for a given antenna pointing error of the listed parameters. The program was implemented in Visual Basic for Application. Sample numerical examples were used to demonstrate the applicability of the program in conducting such parametric analysis.

References

1. Dinc, E., & Akan, O. B. (2014). Beyond-line-of-sight communications with ducting layer. *IEEE communications magazine*, *52*(10), 37-43.
2. Kerczewski, R. J., Wilson, J. D., & Bishop, W. D. (2014, April). Assessing spectrum compatibility for beyond-line-of-sight UAS control and non-payload communications. In *2014 Integrated Communications, Navigation and Surveillance Conference (ICNS) Conference Proceedings* (pp. K2-1). IEEE.
3. Liu, P., Di Renzo, M., & Springer, A. (2016). Line-of-sight spatial modulation for indoor mmWave communication at 60 GHz. *IEEE Transactions on Wireless Communications*, *15*(11), 7373-7389.
4. Immadi, G., Venkata Narayana, M., Kotamraju, S. K., & Sree Madhuri, A. (2018). Estimating the performance of free space optical link under adverse weather conditions by using various models. *Wireless Personal Communications*, *103*(2), 1603-1613.
5. Lee, Y., & Choi, J. P. (2019). Performance evaluation of high-frequency mobile satellite communications. *IEEE Access*, *7*, 49077-49087.
6. Diba, F. D., Afullo, T. J., & Alonge, A. A. (2016). Rainfall rate and attenuation performance analysis at microwave and millimeter bands for the design of terrestrial line-of-sight radio links in Ethiopia. *SAIEE Africa Research Journal*, *107*(3), 177-186.
7. Göktaş, P., Altvntaş, A., Topçu, S., & Karaşan, E. (2014, August). The effect of terrain roughness in the microwave line-of-sight multipath fading estimation based on Rec. ITU-R P. 530-15. In *2014 XXXIth URSI General Assembly and Scientific Symposium (URSI GASS)* (pp. 1-4). IEEE.
8. Rundstedt, K. (2015). *Measurements and channel modelling of microwave line-of-sight MIMO links* (Master's thesis).
9. Yoshida, S., Hasegawa, N., & Kawasaki, S. (2015). Experimental demonstration of microwave power transmission and wireless communication within a prototype reusable spacecraft. *IEEE Microwave and Wireless Components Letters*, *25*(8), 556-558.
10. Sun, S., Thomas, T. A., Rappaport, T. S., Nguyen, H., Kovacs, I. Z., & Rodriguez, I. (2015, December). Path loss, shadow fading, and line-of-sight probability models for 5G urban macro-cellular scenarios. In *2015 IEEE Globecom Workshops (GC Wkshps)* (pp. 1-7). IEEE.
11. Hsiao, A. Y., Yang, C. F., Wang, T. S., Lin, I., & Liao, W. J. (2017, July). Ray tracing simulations for millimeter wave propagation in 5G wireless communications. In *2017 IEEE International Symposium on Antennas and*

Propagation & USNC/URSI National Radio Science Meeting (pp. 1901-1902). IEEE.

12. Ren, Y., Li, L., Xie, G., Yan, Y., Cao, Y., Huang, H., ... & Willner, A. E. (2017). Line-of-sight millimeter-wave communications using orbital angular momentum multiplexing combined with conventional spatial multiplexing. *IEEE Transactions on Wireless Communications*, *16*(5), 3151-3161.
13. Dhillon, H. S., & Caire, G. (2014, June). Scalability of line-of-sight massive MIMO mesh networks for wireless backhaul. In *2014 IEEE International Symposium on Information Theory* (pp. 2709-2713). IEEE.
14. Frid, H., Holter, H., & Jonsson, B. L. G. (2015). An approximate method for calculating the near-field mutual coupling between line-of-sight antennas on vehicles. *IEEE Transactions on Antennas and Propagation*, *63*(9), 4132-4138.
15. Khalife, J., Kassas, Z., & Saab, S. (2015, September). Indoor localization based on floor plans and power maps: Non-line of sight to virtual line of sight. In *Proceedings of ION GNSS Conference* (pp. 2291-2300).
16. Tekbıyık, K., Ulusoy, E., Ekti, A. R., Yarkan, S., Baykaş, T., Görçin, A., & Kurt, G. K. (2019, September). Statistical channel modeling for short range line–of–sight terahertz communication. In *2019 IEEE 30th Annual International Symposium on Personal, Indoor and Mobile Radio Communications (PIMRC)* (pp. 1-5). IEEE.
17. Yan, Y., Bondalapati, P., Tiwari, A., Xia, C., Cashion, A., Zhang, D., ... & Reed, M. (2018, December). 11-Gbps broadband modem-agnostic line-of-sight MIMO over the range of 13 km. In *2018 IEEE Global Communications Conference (GLOBECOM)* (pp. 1-7). IEEE.
18. Khan, M., Bhunia, S., Yuksel, M., & Kane, L. C. (2018). Line-of-sight discovery in 3D using highly directional transceivers. *IEEE Transactions on Mobile Computing*, *18*(12), 2885-2898.
19. Yoo, S. K., Cotton, S. L., Chun, Y. J., Scanlon, W. G., & Conway, G. A. (2017). Channel characteristics of dynamic off-body communications at 60 GHz under line-of-sight (LOS) and non-LOS conditions. *IEEE Antennas and Wireless Propagation Letters*, *16*, 1553-1556.
20. Palizban, N. (2017). *Millimeter wave small cell network planning for outdoor line-of-sight coverage* (Doctoral dissertation, Carleton University).
21. Dinc, E., & Akan, O. B. (2014). Beyond-line-of-sight communications with ducting layer. *IEEE communications magazine*, *52*(10), 37-43.
22. Femi-Jemilohun, O. J., Quinlan, T., Barc, S., & Walker, S. D. (2014). An experimental investigation into GbE wireless data communication at 24 GHz in non-line-of-sight and multipath rich environments. *IEEE Antennas and Wireless Propagation Letters*, *13*, 1219-1222.
23. McCrink, M., & Gregory, J. W. (2018). Design and development of a high-speed uas for beyond line-of-sight operation. In *2018 AIAA Information Systems-AIAA Infotech@ Aerospace* (p. 0750).
24. Hansryd, J., Edstam, J., Olsson, B. E., & Larsson, C. (2014). Non-line-of-sight microwave backhaul for small cells. *Celebrating 90 years of technology insights*, 12.
25. Griner, J. H., & Kerczewski, R. J. (2017, April). Communications for UAS integration in the NAS phase 2-satellite communications and terrestrial extension. In *2017 Integrated Communications, Navigation and Surveillance Conference (ICNS)* (pp. 4A4-1). IEEE.
26. Fraire, J. A., Céspedes, S., & Accettura, N. (2019, October). Direct-to-satellite IoT-A survey of the state of the art and future research perspectives. In *International Conference on Ad-Hoc Networks and Wireless* (pp. 241-258). Springer, Cham.
27. Zeng, Y., Clerckx, B., & Zhang, R. (2017). Communications and signals design for wireless power transmission. *IEEE Transactions on Communications*, *65*(5), 2264-2290.
28. Ippolito Jr, L. J. (2017). *Satellite communications systems engineering: atmospheric effects, satellite link design and system performance*. John Wiley & Sons.
29. Sharma, M., Parini, C. G., & Alomainy, A. (2015, April). Influence of antenna alignment and line-of-sight obstruction on the accuracy of range estimates between a pair of miniature UWB antennas. In *2015 9th European Conference on Antennas and Propagation (EuCAP)* (pp. 1-5). IEEE.
30. Catherwood, P. A., Hughes, P., & McLaughlin, J. (2019). Low-cost RF 802.11 g telemetry for flight guidance system development. *The Journal of Engineering*, *2019*(12), 8496-8503.
31. Mei, H., Yang, X., Han, B., & Tan, G. (2016). High-efficiency microstrip rectenna for microwave power transmission at Ka band with low cost. *IET Microwaves, Antennas & Propagation*, *10*(15), 1648-1655.

32. Zhang, H., Gao, S. P., Ngo, T., Wu, W., & Guo, Y. X. (2019). Wireless power transfer antenna alignment using intermodulation for two-tone powered implantable medical devices. *IEEE Transactions on Microwave Theory and Techniques*, *67*(5), 1708-1716.
33. Kunz, J., & Kim, E. (2015, October). Achieving impressive global positioning and stability in a high fidelity antenna measurement system. In *AMTA 2015 Proceedings* (pp. 320-325).
34. Gonzalez-Prelcic, N., Méndez-Rial, R., & Heath, R. W. (2016, January). Radar aided beam alignment in mmWave V2I communications supporting antenna diversity. In *2016 Information Theory and Applications Workshop (ITA)* (pp. 1-7). IEEE.
35. Zhang, J., Huang, J., Zhou, J., Wang, C., & Zhu, Y. (2016). A compensator for large antennas based on pointing error estimation under a wind load. *IEEE Transactions on Control Systems Technology*, *25*(5), 1912-1920.
36. Zhang, J., Huang, J., Qiu, L., & Song, R. (2015). Analysis of Reflector Vibration-Induced Pointing Errors for Large Antennas Subject to Wind Disturbance: Evaluating the pointing error caused by reflector deformation. *IEEE Antennas and Propagation Magazine*, *57*(6), 46-61.
37. Zhang, J., Huang, J., Wang, S., & Wang, C. (2015). An active pointing compensator for large beam waveguide antenna under wind disturbance. *IEEE/ASME Transactions on Mechatronics*, *21*(2), 860-871.
38. Zhang, J., Huang, J., Liang, W., Zhang, Y., Xu, Q., Yi, L., & Wang, C. (2018). A correction method of estimating the pointing error for reflector antenna. *Shock and Vibration*, *2018*.
39. Devika, S. V., KARKI, K., KOTAMRAJU, S. K., Kavya, K., & RAHMAN, M. Z. (2017). A NEW COMPUTATION METHOD FOR POINTING ACCURACY OF CASSEGRAIN ANTENNA IN SATELLITE COMMUNICATION. *Journal of Theoretical & Applied Information Technology*, *95*(13).
40. Qiuqiu, W. E. N., Tianyu, L. U., Qunli, X. I. A., & Zedong, S. U. N. (2017). Beam-pointing error compensation method of phased array radar seeker with phantom-bit technology. *Chinese Journal of Aeronautics*, *30*(3), 1217-1230.
41. Kavya, K. C. H. S. R. I., Kotamraju, S. K., Kumar, B. N., Mounika, M. D. N. S., Singh, S. R. O. T. E., & SIDDA, A. (2017). Beam pointing accuracy of phased arrays for satellite communication. *Journal of Theoretical and Applied Information Technology*, *95*(10), 2170-2181.
42. Zhang, J., Huang, J., Zhao, P., Liang, W., Zhang, Y., & Wang, C. (2019). A pointing error analysis model for large reflector antennas under wind disturbance. *Proceedings of the Institution of Mechanical Engineers, Part C: Journal of Mechanical Engineering Science*, *233*(6), 1939-1951.
43. Liu, Q., Lu, S. N., & Ding, X. L. (2018). An error equivalent model of revolute joints with clearances for antenna pointing mechanisms. *Chinese Journal of Mechanical Engineering*, *31*(1), 1-9.
44. Sayehvand, J., & Amirabadi, M. A. (2018). Performance analysis of hybrid FSO/RF communication systems with Alamouti Coding or Antenna Selection. *arXiv preprint arXiv:1802.07286*.
45. Hu, K. Y., Yusup, A. L., & Xu, Q. (2015). Deformation Measurement and Pointing Model Analysis of 25m Antenna. In *Applied Mechanics and Materials* (Vol. 713, pp. 424-431). Trans Tech Publications Ltd.